Full Wave Calculations of Gravity Wave Propagation through the Thermosphere

H. VOLLAND[1, 2]

Goddard Space Flight Center, Greenbelt, Maryland 20771

Full wave calculations have been performed within the frequency range of gravity waves ($10^{-3} \leq \omega \leq 10^{-2}$ sec^{-1}) for a thermospheric model between 150 and 500 km altitude. In this altitude range gravity waves are coupled with heat conduction waves. Reflection, transmission, conversion, and coupling from one wave type into the other one is described by the elements of the scattering matrix. The dependence of these elements on height and angle of incidence is discussed. The transmission coefficients of gravity waves calculated by full wave theory are compared with simple ray calculations and show that ray treatment is a sufficient approximation for obliquely upward propagating gravity waves and that gravity waves predominate throughout the thermosphere. The thermosphere reacts like a selective filter with respect to upward propagating gravity waves with optimal transmission at $k_x \sim \omega/C$ (ω = angular frequency; C = velocity of sound; k_x = horizontal wave number).

INTRODUCTION

Satellite drag measurements of the neutral air density [*Jacchia*, 1959; *Priester*, 1959] have revealed for the first time that large-scale diurnal variations of the density in thermospheric heights between 150 and at least 1200 km altitude exist, thermally driven by EUV heating from the sun [*Harris and Priester*, 1962]. *Hines* [1960] put forward the hypothesis that free internal gravity waves of smaller periods generated within the lower atmosphere can propagate into the thermosphere. He suggested that traveling ionospheric disturbances observed within the *F region* [see, e.g., *Heisler*, 1967] are the response of the ionospheric plasma to these neutral air waves. Theoretical calculations, especially those dealing with the ionospheric effect of the Russian H-bomb explosion of October 30, 1961 [*Kohl*, 1964; *Row*, 1967; *Hines*, 1967], show surprisingly good agreement between the observed variations of the *F*-layer critical frequency at different stations and the theoretically expected dispersion effect of internal gravity waves depending on angle of incidence. *Hines* [1967] could even explain the apparent period of the disturbance by a simple ray approach of the direction of energy propagation of gravity waves.

Recently, radar backscatter measurements [*Thome*, 1964] and HF Doppler-effect measurements [*Georges*, 1968] as well as neutral air density observations by pressure gage measurements on board Explorer 32 [*Newton et al.*, 1969] have shown that wave-like structure in the thermosphere with periods of the order of ½ hour reaches altitudes as high as 600 km. *Hines* [1968] and *Newton et al.* [1969], using a ray treatment, explained these waves again as free internal gravity waves propagating from the lower atmosphere up into the thermosphere. The most striking feature of these large altitude waves is the bending of the wave normals toward a horizontal direction with increasing altitude. In a ray treatment this bending is a dispersion effect due to energy dissipation of the waves [*Hines*, 1968; *Newton et al.*, 1969].

From the work of *Harris and Priester* [1962] and of *Pitteway and Hines* [1963] it can be suggested that heat conductivity is of predominating influence for the energy dissipation of neutral air waves. It can be shown numerically that the coefficient of viscosity can be neglected as compared with heat conductivity in thermospheric heights below 600 km and within the frequency range of gravity waves [*Volland*, 1969].

Under the influence of heat conduction, two different pairs of wave modes exist within the thermosphere: acoustic-gravity waves and heat conduction waves. They are coupled with each

[1] Present address: Astronomical Institutes, University of Bonn, Germany.

[2] NAS-NRC Associate with NASA.

other at any height because their eigenvalues depend on the ratio

$$\frac{\kappa}{\langle p \rangle}$$

(κ = coefficient of heat conduction; $\langle p \rangle$ = mean pressure) which increases with height, and therefore the thermosphere behaves like an inhomogeneous medium. Heat conduction waves are evanescent waves below about 200 km altitude. At higher altitudes, however, their attenuation rate is of the same order of magnitude as the attenuation rate of gravity waves. For these two reasons, the response of the thermosphere to the different wave modes including coupling and reflection processes must be determined by a full wave treatment, and a ray approximation has to be justified by these exact calculations.

Full wave calculations of neutral atmospheric waves at altitudes below 200 km have been performed by *Midgley and Liemohn* [1966]. They calculated reflection coefficients of gravity waves and eliminated the evanescent heat conduction waves and viscosity waves by a special mathematical technique.

As pointed out above, this technique, which is fully justified at altitudes below 200 km, is not acceptable at greater heights because there heat conduction waves are no longer of an evanescent type.

This paper deals with a full wave treatment of neutral atmospheric waves at thermospheric heights taking into account heat conduction but neglecting viscosity, ion drag, and Coriolis force. The negligence of the coefficient of viscosity is allowed at heights below 600 km and within the frequency range of gravity waves ($\omega \lesssim 10^{-2}$ sec^{-1}). The negligence of ion drag and Coriolis force is possible at frequencies

$$\omega > \begin{cases} \nu \\ 2\Omega \end{cases}$$

where $\Omega = 7.3 \times 10^{-5}$ sec^{-1} is the rotation period of the earth and ν is the collision frequency between one neutral and the ions. The maximum collision frequency ν within the F_2 layer is of the order of $\nu \lesssim 5 \times 10^{-4}$ sec^{-1}. The validity of our numerical calculations, therefore, is limited to an altitude range of $100 \leqq z \leqq 500$ km and a frequency range of $10^{-2} < \omega < 10^{-3}$ sec^{-1}, which is the range of gravity waves. We shall compare these full wave calculations with simple ray approximation and shall mark the range of horizontal wave numbers where a ray treatment is a sufficient approximation for gravity wave propagation.

Theory

Since we deal with gravity waves of periods $10^{-2} < \omega < 10^{-3}$ sec^{-1} at heights below 600 km we can neglect the coefficient of viscosity, ion drag, and Coriolis force. We moreover consider only the simplest wave form, namely, plane, free interval, harmonic waves of angular frequency ω propagating obliquely into a quiet horizontally stratified, isothermal atmosphere. The parameters of the atmosphere are only functions of altitude z. The propagation plane shall be the $(x - z)$ plane of a Cartesian coordinate system. A strict perturbation method then leads to a system of first-order differential equations [*Volland*, 1969]

$$d\mathbf{e}/dz = jk\mathbf{K}\mathbf{e} \tag{1}$$

where

$$\mathbf{e}(z) = \begin{bmatrix} e_1 \\ e_2 \\ e_3 \\ e_4 \end{bmatrix} \tag{2}$$

$$e_1 = \left(\frac{\langle p \rangle}{C}\right)^{1/2} \Delta w$$

$$e_2 = \left(\frac{C}{\langle p \rangle}\right)^{1/2} \Delta p$$

$$e_3 = \frac{(\langle p \rangle C)^{1/2}}{\langle T \rangle} \Delta T$$

$$e_4 = \frac{\kappa}{(\langle p \rangle C)^{1/2}} \frac{d\Delta T}{dz}$$

$$\Delta u = \left(\frac{C}{\langle p \rangle}\right)^{1/2} \frac{S}{\gamma} e_2$$

$$\Delta \rho = \frac{\langle \rho \rangle}{(\langle p \rangle C)^{1/2}} (e_2 - e_3)$$

Δu horizontal velocity
Δw vertical velocity
Δp = wave amplitudes of pressure
ΔT temperature
$\Delta \rho$ density

C acoustic phase velocity

$\langle p\rangle(z)$ = time independent pressure
$\langle T\rangle$ values of temperature
$\langle\rho\rangle(z)$ density

$$\mathbf{K}(z) = \begin{bmatrix} -jA & -\left(1 - \frac{S^2}{\gamma}\right) & 1 & 0 \\ -\gamma & jA & -2jA & 0 \\ 0 & 0 & jA & \frac{-2jG}{d} \\ -2jA & -1 & d\left(1 + \frac{S^2}{2jG}\right) & -jA \end{bmatrix}$$

κ = coefficient of heat conductivity.
γ = c_p/c_v, ratio of specific heats at constant pressure and constant volume.
S = k_x/k, normalized horizontal wavenumber.
k_x = horizontal wave number in x direction considered as real and constant.
k = ω/C, wave number of acoustic waves.
ω = angular frequency considered as real and constant.
C = $[\gamma(R/M)\langle T\rangle]^{1/2}$ acoustic phase velocity.
R = gas constant.
M = molecular weight.
A = ω_a/ω.
G = ω_b/ω.
d = $[\gamma/(\gamma - 1)]$.
ω_a = $\gamma g/2C$.
ω_b = $\gamma g/2V$.
V = $\kappa g/c_p\langle p\rangle$, heat conduction velocity.
g = gravitational acceleration.

The wave amplitudes of horizontal velocity Δu and of density $\Delta\rho$ are linearly related with e_2 and e_3 and do not appear explicitly in system equation 1.

The height dependence of $\mathbf{K}$ in equation 1 within an isothermal atmosphere is due only to the parameter $G(z)$ because κ = constant, but

$$p = p_0 e^{-z/H}$$

We define a homogeneous isothermal atmosphere by the condition G = constant, which implies

$$p \propto \kappa = \kappa_0 e^{-z/H} \tag{3}$$

and we shall approximate the real atmosphere by a number of such homogeneous isothermal slabs.

Four characteristic waves, two gravity waves and two heat conduction waves, can propagate within a homogeneous isothermal thermosphere in which heat conduction is taken into account and equation 3 holds. Their vertical propagation characteristics are described by the formula

$$\mathbf{c} = \begin{bmatrix} a_G \\ a_H \\ b_G \\ b_H \end{bmatrix} = \mathbf{c}_0 e^{jk\mathbf{N}z} \tag{4}$$

where the column matrix $\mathbf{c}$ contains the four wave modes,

$$e^{jk\mathbf{N}z} = \begin{bmatrix} e^{-jkq_G z} & 0 & 0 & 0 \\ 0 & e^{-jkq_H z} & 0 & 0 \\ 0 & 0 & e^{jkq_G z} & 0 \\ 0 & 0 & 0 & e^{jkq_H z} \end{bmatrix} \tag{5}$$

and $\mathbf{N}$ is a diagonal matrix with the eigenvalues of the matrix $\mathbf{K}$ in its diagonal

$$q_i = \left\{\frac{\gamma}{2} - A^2 - S^2 - jG \mp \left[\left(\frac{\gamma}{2} - jG\right)^2 + 2jG(1 + B^2S^2)\right]^{1/2}\right\}^{1/2} \tag{6}$$

with

$$B = 2\frac{[(\gamma - 1)]^{1/2}}{\gamma} \quad A = \frac{\omega_b}{\omega}$$

(ω_b = Brunt-Vaisälä frequency)
[see *Pitteway and Hines*, 1963, equation 36]. The minus sign within the square-root of the eigenvalue equation 6 is associated with the pair of acoustic-gravity waves (an ascending one ($c_1 = a_G$) and a descending one ($c_3 = b_G$)). The plus sign is associated with the equivalent heat conduction waves ($c_2 = a_H$; $c_4 = b_H$). The term 'upgoing' means that the wave transports energy upward. This implies a negative imaginary term of q_i. A downgoing wave has then a positive imaginary part of q_i.

In the case of a loss-free atmosphere, in which heat conduction is zero, the eigenvalue equation 6 reduces to the well-known equation of gravity waves [*Hines*, 1960]

$$q_G = [1 - A^2 - S^2(1 - B^2)]^{1/2} \tag{7}$$

while $q_H \to \infty$ indicates that heat conduction waves become evanescent waves.

The characteristic waves are related with the physical parameters **e** of equation 2 by

$$\mathbf{e} = \mathbf{Qc} \tag{8}$$

where **Q** can be found from the condition

$$\mathbf{KQ} = \mathbf{QN}$$

as

$$Q_{ki} = L_{ki}\left[\frac{2}{\mathrm{Re}\,(q_i)(\gamma - 4S^2A^2/\gamma)}\right]^{1/2} \tag{9}$$

with

$$L_{1i} = q_i - jA\left(1 - \frac{2S^2}{\gamma}\right)$$

$$L_{2i} = \gamma - 2A^2 - 2jAq_i$$

$$L_{3i} = \gamma - S^2 - A^2 - q_i^2$$

$$L_{4i} = \frac{dL_{3i}}{2jG}\,(q_i + jA)$$

The characteristic waves are normalized in such a manner that

$$c_i c_i^* = \tfrac{1}{2}\,\mathrm{Re}\,(\Delta w_i\,\Delta p_i^*) \tag{10}$$

gives the time-averaged vertical energy flux of the ith characteristic wave. (The star indicates conjugate complex values.)

If we divide the realistic atmosphere into a number of homogeneous isothermal slabs of thickness Δz_m, equations 1 and 4 lead in a straightforward manner to the solution

$$\mathbf{c}^{II} = \mathbf{P}_I^{II}\mathbf{c}^I \tag{11}$$

with

$$\mathbf{c}^I = \mathbf{c}(z_I)$$

$$\mathbf{c}^{II} = \mathbf{c}(z_{II})$$

$$\mathbf{P}_I^{II} = \prod_{m=1}^{n} e^{jk_m\mathbf{N}_m\Delta z_m}\mathbf{Q}_m^{-1}\Gamma_m\mathbf{Q}_{m-1}$$

and

$$\Gamma_m = \left(\frac{C_m}{C_{m-1}}\right)^{1/2} \cdot \begin{bmatrix} C_{m-1}/C_m & 0 & 0 & 0 \\ 0 & 1 & 0 & 0 \\ 0 & 0 & T_{m-1}/T_m & 0 \\ 0 & 0 & 0 & C_{m-1}/C_m \end{bmatrix}$$

The matrix Γ_m matches the internal boundary condition of continuous wave amplitudes of Δw, Δp, ΔT, and $\kappa d\,(\Delta T)/dz$ between two adjacent slabs of temperatures T_{m-1} and T_m.

Ray approximation assumes that reflection and coupling between the different characteristic waves are negligibly small and that the height dependence of the ith characteristic wave can be described by

$$c_i(z_{II}) = P_{Ri}c_i(z_I) \tag{12}$$

with

$$P_{Ri} = \exp\left\{-j\int_{z_I}^{z_{II}} kq_i(\xi)\,d\xi\right\}$$

which is equivalent to

$$\mathbf{P}_I^{II} \to \exp\left\{j\int_{z_I}^{z_{II}} k\mathbf{N}\,d\xi\right\} = \begin{bmatrix} P_{R1} & 0 & 0 & 0 \\ 0 & P_{R2} & 0 & 0 \\ 0 & 0 & 1/P_{R1} & 0 \\ 0 & 0 & 0 & 1/P_{R2} \end{bmatrix} \tag{13}$$

in equation 11.

The Elements of the Scattering Matrix

As shown in the preceding section, two pairs of characteristic waves exist within the neutral thermosphere which we collected by a column matrix (see equation 4), where a_G, b_G are ascending and descending gravity waves, respectively, and a_H, b_H are ascending and descending heat conduction waves, respectively.

Our model atmosphere consists of three regions (see Figure 1). The regions below z_I (region I) and above z_{II} (region III) are considered as homogeneous (G = constant) and isothermal ($\langle T\rangle$ = constant) atmospheres extended infinitely into the half spaces. The region between z_I and z_{II} (region II) approximates part of the real atmosphere. Its parameters approach the parameters of regions I and III at the boundaries z_I and z_{II}, respectively.

Coupling between the four characteristic waves then only occurs within region II, whereas in regions I and III the waves are uncoupled with each other. The connection between the four waves at the lower boundary

z_I with the four waves at the upper boundary z_{II} of region II is given by equation 11.

We are mainly interested in reflection and transmission of gravity waves. This can be described by the elements of the scattering matrix, well known in electromagnetic wave propagation [see, e.g., *Volland*, 1962]. The scattering matrix connects the waves going into region II with the waves coming out of region II

$$\begin{aligned} \mathbf{b}^{I} &= \mathbf{R}^{I}\mathbf{a}^{I} + \mathbf{T}^{II}\mathbf{b}^{II} \\ \mathbf{a}^{II} &= \mathbf{T}^{I}\mathbf{a}^{I} + \mathbf{R}^{II}\mathbf{b}^{II} \end{aligned} \tag{14}$$

where we introduced column matrices of ascending and descending waves

$$\mathbf{a} = \begin{bmatrix} a_G \\ a_H \end{bmatrix} \qquad \mathbf{b} = \begin{bmatrix} b_G \\ b_H \end{bmatrix}$$

$\mathbf{R}^{I}$ and $\mathbf{R}^{II}$ are (2×2), reflection matrices; and $\mathbf{T}^{I}$ and $\mathbf{T}^{II}$ are (2×2), transmission matrices. We collect these last four matrices into a (4×4) scattering matrix

$$\mathbf{S}_I^{II} = \begin{bmatrix} \mathbf{R}^{I} & \mathbf{T}^{II} \\ \mathbf{T}^{I} & \mathbf{R}^{II} \end{bmatrix} \tag{15}$$

A simple algebraic transformation leads to relations between the submatrices of $\mathbf{S}_I^{II}$ and the submatrices of $\mathbf{P}_I^{II}$ in equation 11

$$\begin{aligned} \mathbf{R}^{I} &= -\mathbf{P}_4^{-1}\mathbf{P}_3 \\ \mathbf{R}^{II} &= \mathbf{P}_2\mathbf{P}_4^{-1} \\ \mathbf{T}^{I} &= \mathbf{P}_1 - \mathbf{P}_2\mathbf{P}_4^{-1}\mathbf{P}_3 \\ \mathbf{T}^{II} &= \mathbf{P}_4^{-1} \end{aligned} \tag{16}$$

where

$$\mathbf{P}_I^{II} = \begin{bmatrix} \mathbf{P}_1 & \mathbf{P}_2 \\ \mathbf{P}_3 & \mathbf{P}_4 \end{bmatrix}$$

The elements of $\mathbf{S}_I^{II}$ completely describe the behavior of region II with respect to plane waves. It is, e.g.,

$$\mathbf{R}^{I} = \begin{bmatrix} {}_G\mathbf{R}_G^{I} & {}_G\mathbf{R}_H^{I} \\ {}_H\mathbf{R}_G^{I} & {}_H\mathbf{R}_H^{I} \end{bmatrix} \tag{17}$$

where the elements ${}_G\mathbf{R}_G^{I}$ and ${}_H\mathbf{R}_H^{I}$ are related to the reflection of gravity waves (G) or heat conduction waves (H) coming from below. ${}_H\mathbf{R}_G^{I}$ and ${}_G\mathbf{R}_H^{I}$ are conversion coefficients transferring part of the incoming wave energy of one wave type into reflected wave energy of the other wave type. Equivalent relations hold for the other three submatrices $\mathbf{R}^{II}$, $\mathbf{T}^{I}$, and $\mathbf{T}^{II}$.

Figure 1 shows the four elements of the first column of matrix $\mathbf{S}_I^{II}$ (equation 15), which give the ratios between reflected and transmitted waves, respectively, and an incoming gravity wave from below.

Twelve equivalent elements for the three other incoming waves exist but are only outlined in Figure 1.

Wave Energy and Wave Amplitude

The characteristic waves are normalized in such a manner that $a_i\, a_i^*$ (or $b_i\, b_i^*$) give the time-averaged vertical energy flow of the ith wave. Therefore, $R\, R^*$ (or $T\, T^*$) is the ratio between the reflected (or transmitted) vertical energy flux to the incoming vertical energy flux. The definition of vertical energy flux (equation 10) is based on the classical formula of nondissipative waves within an adiabatically behaving atmosphere. It is approximately valid also for dissipative waves, where part of the wave energy is transferred into internal energy

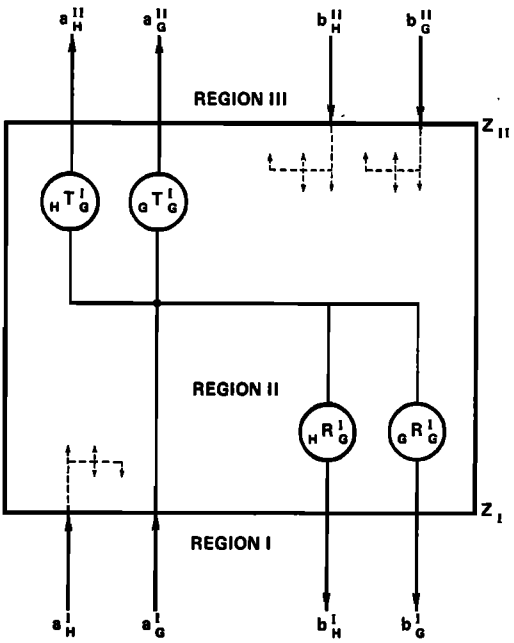

Fig. 1. Elements of the scattering matrix. Reflection coefficients (R) and transmission coefficients (T) of upward (a) and downward (b) propagating gravity waves (G) and heat conduction waves (H) within the thermosphere.

of the surrounding gas by heat conductivity, as long as the gravity waves belong to the type of propagation waves. If, however, the incoming gravity wave is of an evanescent type, where the real part of the eigenvalue disappears, the energy definition of equation 10 breaks down.

At 150 km height, the lower boundary of our model, gravity waves behave nearly like nondissipative waves. From the eigenvalue equation of nondissipative gravity waves (equation 7) we can immediately find the horizontal wave number k_{x0}, which separates propagation waves from evanescent waves. It is

$$q_G = \begin{cases} |q_G| & \text{for } S > S_0 \\ -j\,|q_G| & S < S_0 \end{cases}$$

with

$$S_0 = \frac{k_{x0}}{k} = \left(\frac{A^2 - 1}{B^2 - 1}\right)^{1/2} \tag{18}$$

In the frequency range of gravity waves it is $A > B > 1$. Therefore, gravity waves with horizontal wave numbers

$$k_x < S_0 k \tag{19}$$

belong to the evanescent wave type and cannot propagate near or below 150 km altitude. This range of horizontal wave numbers must be excluded in our calculations.

From a practical point of view it is interesting to know the answer to the following question: Given a relative pressure (or temperature) amplitude of an upgoing gravity wave at a certain height z_I. How does the relative pressure (temperature) amplitude change with height if we take into account reflection and coupling into heat conduction waves?

In this case, downgoing waves at the upper boundary of our model at z_{II} do not exist ($\mathbf{b}^{II} = 0$ in Figure 1), and it is (see equations 2, 8, and 14)

$$\mathbf{y}^{II} = \left(\frac{C_I\langle p_I\rangle}{C_{II}\langle p_{II}\rangle}\right)^{1/2} \mathbf{Q}^{II}\mathbf{P}_I^{II} \cdot \begin{bmatrix} 1 \\ 0 \\ {}_GR_G^I \\ {}_HR_G^I \end{bmatrix} (Q_{21}^I)^{-1} \frac{\Delta p_I}{\langle p_I\rangle} \tag{20}$$

where the column matrix

$$\mathbf{y}^{II} = \frac{\mathbf{e}^{II}}{(C_{II}\langle p_{II}\rangle)^{1/2}}$$

contains as its second element the relative pressure amplitude at the height z_{II}

$$y_2^{II} = \Delta p_{II}/\langle p_{II}\rangle$$

The wave structure at z_{II} observed as a relative pressure amplitude is the sum of two characteristic waves, the original upgoing gravity wave from the altitude z_I and a heat conduction wave coupled from the gravity wave during its propagation from z_I to z_{II}. Part of the original gravity wave is reflected from the altitude z_I as gravity or as heat conduction wave.

The separation between the different characteristic waves has been lost by this kind of calculation. However, any ambiguity arising from a possible error in the definition of the wave energy has disappeared.

The ray approximation equivalent to equation 20 is (see equations 2, 8, and 12)

$$\frac{\Delta p_{II}}{\langle p_{II}\rangle} = \left(\frac{C_I\langle p_I\rangle}{C_{II}\langle p_{II}\rangle}\right)^{1/2} \frac{Q_{21}^{II}}{Q_{21}^I} P_{R1} \frac{\Delta p_I}{\langle p_I\rangle} \tag{21}$$

The term

$$D = \left(\frac{C_I\langle p_I\rangle}{C_{II}\langle p_{II}\rangle}\right)^{1/2} \tag{22}$$

in equations 20 and 21 gives the well-known adiabatic increase of the relative wave amplitude with altitude within a nondissipative atmosphere. It becomes

$$D = e^{(z_{II} - z_I)/2H}$$

in the case of an isothermal atmosphere.

Atmospheric Model

For the model atmosphere in region II (see Figure 1) we chose the Harris-Priester model 5 at 1200 local time [*CIRA*, 1965]. The lower boundary of region II is $z_I = 150$ km. Below z_I an isothermal atmosphere with the temperature at the height z_I is added as region I. The upper boundary z_{II} serves as parameter running from z_I to 500 km. Region III then is an isothermal atmosphere with the temperature in the height z_{II}.

Note that in order to make regions I and III homogeneous with respect to characteristic

waves the coefficient of heat conductivity κ in these regions must decrease exponentially with altitude like the pressure (see equation 3). As will be seen later this is not a serious limitation for the acceptance of that model because below 150 km heat conduction waves become strongly attenuated (their wave amplitude is attenuated by a factor larger than $1/e = 0.37$ after propagating 1 km in the vertical direction), and gravity wave propagation is only slightly influenced by heat conductivity. The region above 500 km otherwise has no influence on the reflection characteristics of gravity waves.

Region II is approximated by a number of homogeneous isothermal slabs of thickness $\Delta z_r = 1$ km. Again in each slab it is $\kappa/\langle p \rangle =$ constant. Repeated calculations decreasing Δz_r to the value of 100 m did not show significant differences in the results and indicate that our model with slab thickness $\Delta z_r = 1$ km is a sufficient approximation of a realistic atmosphere.

Numerical Results

In this section we shall give numerical results for the elements of the scattering matrix determined from equations 11 and 16.

Figure 2*a* gives the magnitude versus height z_{II} of the four elements ${}_GR_G^I$, ${}_HR_G^I$, ${}_GT_G^I$, and ${}_HT_G^I$, which describe reflection, conversion, transmission, and coupling into heat conduction waves of incoming gravity waves from below. The frequency used is $\omega = 3 \times 10^{-3}$ sec^{-1} (equivalent to a period of $t = (2\pi/\omega) = 21$ min), and the horizontal wave number used is $k_x = 2.15 \times 10^{-2}$ km^{-1} (equivalent to a horizontal wavelength of $\lambda_x = 2\pi/k_x = 292$ km).

The transmission coefficient ${}_GT_G^I$ decreases in the altitude range from 150 to 500 km by a factor of 185, indicating that only 3×10^{-5} of the original wave energy at 150 km altitude has reached the altitude of 500 km.

The reflection coefficient ${}_GR_G^I$ remains constant at altitudes above 250 km. Its value of 9×10^{-2} is equivalent to a reflected energy of 8×10^{-3} of the incoming energy. The conversion coefficient ${}_HR_G^I$, which converts part of the incoming gravity wave energy into reflected heat conduction wave energy, has the value 3.6×10^{-3} (equivalent to 10^{-5} of the incoming energy) and remains constant above an altitude of 200 km. The constancy of the reflection factors indicates that the region above 250 km has no influence on the reflection characteristics of the atmosphere below 150 km.

The coupling coefficient ${}_HT_G^I$, which is responsible for the transfer of energy from the gravity mode into heat conduction mode never exceeds 6% of the magnitude of the transmission coefficient ${}_GT_G^I$. Therefore not more than 4‰ of the gravity wave energy is coupled into heat conduction wave energy. Its value of 2.5×10^{-4} at 500 km altitude is equivalent to a ratio of $6 < 10^{-6}$ of the incoming energy.

The rest of the original wave energy at 150 km height, namely about 99%, is dissipated and transferred into internal energy of the surrounding gas during the propagation of the wave from 150 to 500 km.

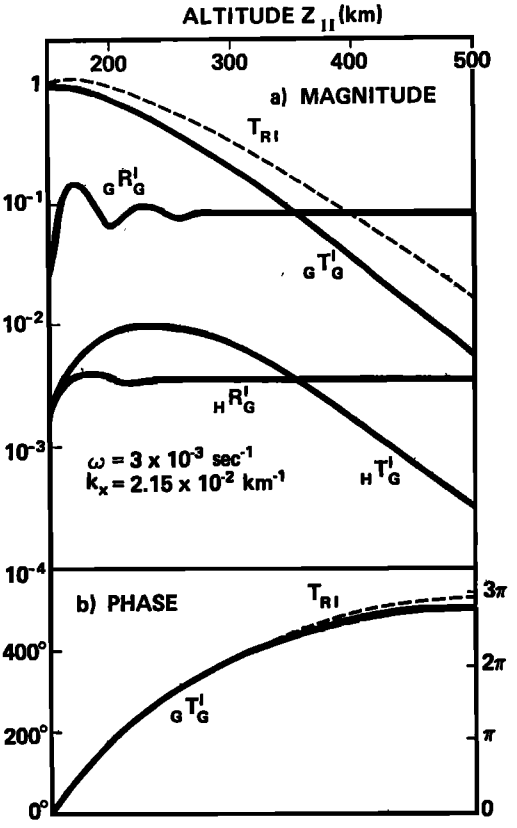

Fig. 2. Magnitude (Figure 2*a*) of coefficients of reflection (${}_GR_G^I$), transmission (${}_GT_G^I$), conversion (${}_HR_G^I$), and coupling (${}_HT_G^I$) into heat conduction waves of upward propagating gravity waves versus z_{II}. Figure 2*b* shows phase of ${}_GT_G^I$. Dashed curves have been calculated from ray theory.

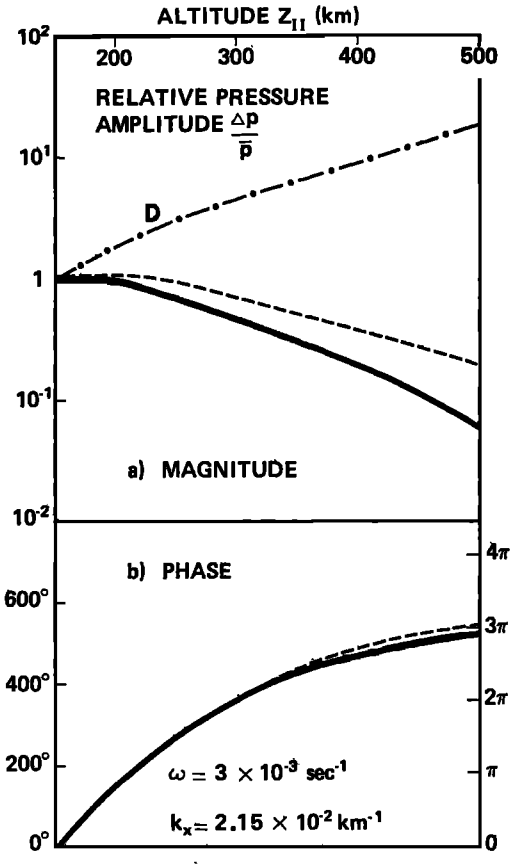

Fig. 3. Magnitude (Figure 3*a*) and phase (Figure 3*b*) of relative pressure amplitude of upward propagating gravity waves calculated by full wave theory (full lines) and by ray approximation (dashed lines). The dash-dotted line represents the adiabatic increase of the amplitude of a nondissipative wave.

Figure 2*b* shows the phase of the transmission coefficient ${}_GT_G^I$. We note that the thickness of the thermosphere in terms of vertical wavelengths of gravity waves is only of the order of one wavelength. The dashed lines in Figure 2 give the transmission coefficient $T_{R1} = P_{R1}$ calculated from ray approximation (equation 12). We observe a very small difference between the phases of ${}_GT_G^I$ and T_{R1}, but a ratio of the magnitudes increasing to the value of

$$\left| \frac{T_{R1}}{{}_GT_G^I} \right| = 3.1 \qquad (23)$$

at 500 km height. Thus, ray approximation leads to a too large magnitude of the transmission coefficient, but to a sufficiently correct phase.

In Figure 3 the relative pressure amplitudes calculated from full wave theory (equation 20) (solid lines) and from ray theory (equation 21) (dashed lines) have been plotted versus z_{II}. The pressure amplitudes are related to the amplitude $\Delta p_I/\langle p_I \rangle = 1$ at 150 km altitude. The dash-dotted line in Figure 3*a* represents the factor D (equation 22), which is the adiabatic increase of the relative pressure amplitude with height of a nondissipative wave. The ratio between the relative pressure amplitudes calculated from ray theory and from full wave theory at 500 km altitude is nearly the same as the ratio of the transmission coefficients (equation 23). Comparing equations 11, 12, 20, and 21 we conclude, therefore, that reflection and coupling has a negligibly small influence on gravity wave propagation in these ranges of frequency and horizontal wavenumber.

The relative pressure amplitude in Figure 3*a* (dashed line) is smaller by a factor of 10^{-2} than the pressure amplitude of the adiabatic wave at 500 km height (dash-dotted line in Figure 3*a*). We compare this number with the magnitude of the transmission coefficient which we find from Figure 2*a* (dashed line) as 1.5×10^{-2}. We notice that the pressure amplitude decreases stronger than the transmission coefficients predicts. From equation 21 it follows that this is the result of the height dependent coefficient $Q_{21}(z)$ of the transformation matrix $\mathbf{Q}$ in equation 8.

In Figure 4 the four elements ${}_GR_G^I$, ${}_HR_G^I$, ${}_GT_G^I$, and ${}_HT_G^I$ discussed in Figure 2 have been calculated for a region II ranging from 150 to 500 km and are plotted versus horizontal wave number k_x. Angular frequency of the wave is again $\omega = 3 \times 10^{-3}$ sec^{-1}. Lower limit of the wave number is the value $S_0 \sim 1$ (see equation 18), which is related to the height $z_I = 150$ km. At $S < S_0$ gravity waves belong to the evanescent waves and do not exist below 150 km. A layer, in which $S \leqq S_0$, totally reflects adiabatic gravity waves. The calculated reflection coefficient ${}_GR_G^I$, in fact, approaches the value 1 at $S = S_0$. However, Figure 4 shows that the transmission coefficients do not approach zero at $S = S_0$ as one would expect from the definition of reflection and transmission coefficients. This discrepancy is due to the breakdown of our energy definition (equation 10) at $S \lesssim S_0$. In that range of horizontal wave numbers one can

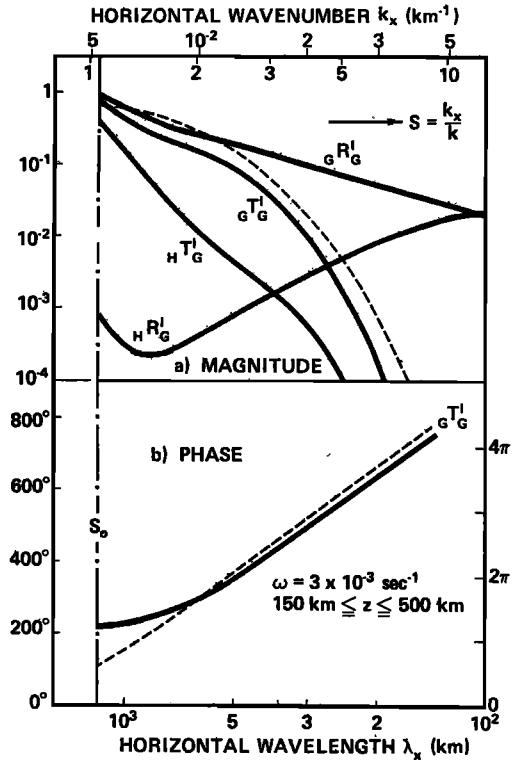

Fig. 4. Magnitude (Figure 4*a*) of coefficients of reflection, transmission, conversion, and coupling into heat conduction waves of upward propagating gravity waves versus horizontal wave number k_x. Range of thermospheric model: 150 to 500 km. Angular frequency: $\omega = 3 \times 10^{-3}$ sec^{-1}. Figure 4*b* shows phase of $_GT^I_G$; dashed lines have been calculated by ray theory.

only apply equation 20 for the direct determination of the physical wave parameters.

The magnitude of the transmission coefficient in Figure 4 decreases monotonously with increasing S and reaches a value $_GT^I_G \lesssim 10^{-4}$ at $S > 4$. For greater horizontal wavenumbers the atmosphere becomes opaque. Gravity waves can propagate only in the range

$$S_0 \sim 1 < \frac{k_z}{k} < 4$$

with sufficiently small attenuation. The atmosphere, therefore, behaves like a selective filter with respect to gravity waves.

Coupling into heat conduction waves (the element $_HT^I_G$ in Figure 4) is small throughout the whole range of S and can be neglected. Reflection of gravity waves becomes important only near the critical wavenumber S_0.

In Figure 5 the relative pressure amplitude has been calculated for an upgoing gravity wave of frequency $\omega = 3 \times 10^{-3}$ sec^{-1} for the same height range between 150 and 500 km and plotted versus horizontal wavenumber. The monotonously decreasing pressure magnitude truly pictures the decreasing transmission coefficient $_GT^I_G$ of Figure 4. The magnitude reaches a maximum near the critical horizontal wavenumber S_0.

The dashed lines in Figures 4 and 5 have been calculated from ray theory and show that, apart from the region near S_0, the magnitudes of the transmission coefficients calculated from ray theory are larger than the magnitudes calculated by full wave theory. The phases of the transmission coefficients are nearly equal, apart from the region $S < 2$. Ray theory therefore is a

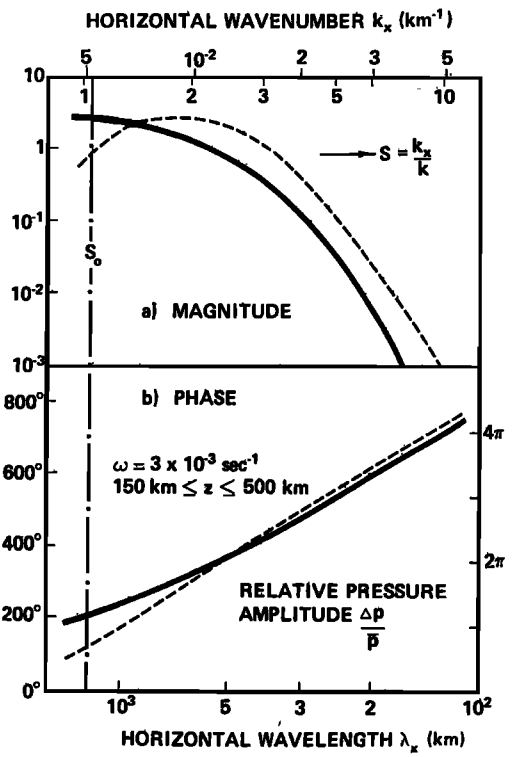

Fig. 5. Magnitude (Figure 5*a*) and phase (Figure 5*b*) of relative pressure amplitude of upward propagating gravity waves versus horizontal wave number. Range of thermospheric model: 150 to 500 km. Angular frequency: $\omega = 3 \times 10^{-3}$ sec^{-1}. Dashed lines have been calculated by ray theory.

sufficient approximation for gravity wave propagation within the thermosphere if one takes into account the differences in magnitude and phase outlined in Figures 4 and 5.

Conclusion

Numerical full wave calculations have been performed within the frequency range of gravity waves ($10^{-3} \leqq \omega \leqq 10^{-2}$ sec^{-1}) in thermospheric heights between 150 and 500 km. In these heights coupling occurs between gravity waves and heat conduction waves. These calculations have been compared with those for simple ray approximation. It has been shown that

(1) Ray treatment is a sufficient approximation for obliquely upward propagating gravity waves at horizontal wave numbers $k_x \gtrsim \omega/C$ (C velocity of sound).

(2) The rate of coupling from gravity wave energy into heat conduction energy is negligibly small for upward propagating gravity waves. Gravity waves, therefore, predominate the upward transport of wave energy within the thermosphere.

(3) The thermosphere reacts like a selective filter with respect to gravity wave. The range of optimal transmission is near $k_x \sim \omega/C$.

References

CIRA, Cospar International Reference Atmosphere, 1965, North-Holland Publishing Company, Amsterdam, 1965.

Georges, T. M., HF Doppler studies of traveling ionospheric disturbances, *J. Atmospheric Terrest. Phys., 30*, 735, 1968.

Harris, I., and W. Priester, Time dependent structure of the upper atmosphere, *J. Atmospheric Sci., 19*, 286, 1962.

Heisler, L. H., Traveling ionospheric disturbances, *Space Res., 7*, 55, 1967.

Hines, C. O., Internal gravity waves in ionospheric heights, *Can. J. Phys., 38*, 1441, 1960.

Hines, C. O., On the nature of traveling ionospheric disturbances launched by low altitude nuclear explosions, *J. Geophys. Res., 72*, 1877, 1967.

Hines, C. O., An effect on molecular dissipation in upper atmospheric gravity waves, *J. Atmospheric Terrest. Phys., 30*, 845, 1968.

Jacchia, L. G., Solar effects on the acceleration of artificial satellites, *Smithsonian Astrophys. Obs. Spec. Rept. No. 29*, 1959.

Kohl, H., Acoustic gravity waves caused by the nuclear explosion on October 30th, 1961, in *Electron Density Distribution in Ionosphere and Exosphere*, edited by E. V. Thrane, p. 160, North-Holland Publishing Company, Amsterdam, 1964.

Midgley, J. E., and H. B. Liemohn, Gravity waves in a realistic atmosphere, *J. Geophys. Res., 71*, 3729, 1966.

Newton, G. P., D. T. Pelz, and H. Volland, Direct, in situ measurements of wave propagation in the neutral thermosphere, *J. Geophys. Res., 74*(1), 183, 1969.

Pitteway, M. L. V., and C. O. Hines, The viscous damping of atmospheric gravity waves, *Can. J. Phys., 71*, 1935, 1963.

Priester, W., Sonnenaktvität and Abbremsung der Erdsatelliten, *Naturwissenschaften, 46, 197*, 1959.

Row, R. V., Localized low altitude sources and acoustic gravity wave perturbations of the ionosphere, paper presented at AGARD 13 Symposium on Phase and Frequency Instability in Electromagnetic Wave Propagation, Ankara, Turkey, October 1967.

Thome, G. D., Incoherent scatter observations of traveling ionospheric disturbances, *J. Geophys. Res., 69*, 4047, 1964.

Volland, H., The propagation of plane electromagnetic waves in a horizontally stratified ionosphere, *J. Atmospheric Terrest. Phys., 24*, 853, 1962.

Volland, H., The upper atmosphere as a multiply refractive medium for neutral air motions, to be published in *J. Atmospheric Terrest. Phys.*, 1969.

(Received June 24, 1968;
revised December 18, 1968.)